Journal of Neurochemistry, 2006, **97**, 30–43 doi:10.1111/j.1471-4159.2006.03705.x

Visualization of APP dimerization and APP-Notch2 heterodimerization in living cells using bimolecular fluorescence complementation

Ci-Di Chen,* Sun-Young Oh,* Jason D. Hinman† and Carmela R. Abraham*,†

*Departments of *Biochemistry and †Medicine, Boston University School of Medicine, Boston, Massachusetts, USA*

Abstract

We previously demonstrated that the amyloid precursor protein (APP) interacts with Notch receptors. Here, we confirmed the APP/Notch1 endogenous interaction in embryonic day 17 rat brain tissue, suggesting the interaction was not as a result of over-expression artifacts. To investigate potential homodimeric and heterodimeric interactions of APP and Notch2 (N2), we have visualized the subcellular localization of the APP/N2 complexes formed in living cells using bimolecular fluorescence complementation (BiFC) analysis. BiFC was accomplished by fusing the N-terminal fragment or the C-terminal fragment of yellow fluorescent protein (YFP) to APP, N2, and a C-terminally truncated form of N2. When expressed in COS-7 cells, these tagged proteins alone did not produce a fluorescent signal. The tagged APP homodimer produced a weak fluorescent signal, while neither full-length N2, nor a truncated N2 alone, produced a visible signal, suggesting that N2 receptors do not form homodimers. The strongest fluorescent signal was obtained with co-expression of the C-terminal fragment of YFP fused to APP and the N-terminal fragment of YFP fused to the truncated form of N2. This heterodimer localized to plasma membrane, endoplasmic reticulum (ER), Golgi and other compartments. The results were confirmed and quantified by flow cytometry. The BiFC method of specifically visualizing APP/Notch interactions can be applied to study APP and Notch signaling during development, aging and neurodegeneration.

Keywords: Alzheimer's disease, Notch signaling, presenilin, immunofluorescence.

J. Neurochem. (2006) **97**, 30–43.

The amyloid precursor protein (APP) is a ubiquitously expressed type I membrane protein. At present, the most well-established functional aspect of APP lies in its proteolytic processing that results in the generation of the amyloid β peptide (Aβ). Aβ is a neurotoxic peptide that plays an important role in the pathogenesis of Alzheimer's disease (Selkoe and Kopan 2003). Many studies were initiated to try to elucidate the biological function of APP, but, as of today, no clear biological function has been revealed. Efforts have been made to identify the physiological functions of APP in mammalian cell culture systems, knockout or transgenic models in mice and nematodes, and by using rapidly advancing proteomics tools. As a result, studies have suggested various functions of this protein including: cell adhesion, cell growth and survival (Weidemann *et al*. 1989), cell migration (Herms *et al*. 2004), neuroprotection (Mucke *et al*. 1995; Masliah *et al*. 1997), synaptotrophism (Mucke *et al*. 1994), synapse remodeling (Ashley *et al*. 2005), axonal transport (Koo *et al*. 1990; Kamal *et al*. 2000), neuronal apoptosis (Rohn *et al*. 2000; Combs *et al*. 2001; Chen *et al*. 2003; Floden *et al*. 2005), protease inhibition (Van Nostrand *et al*. 1990), effects on cellular energy levels and mitochondrial function (Li *et al*. 2005), and involvement in transcription (Gao and Pimplikar 2001; Kimberly *et al*. 2001; Cao and

Received August 29, 2005; accepted November 25, 2005.

Address correspondence and reprint requests to Carmela R. Abraham, Department of Biochemistry and Medicine, Boston University School of Medicine, 715 Albany Street, Boston, MA 02118, USA.
E-mail: cabraham@bu.edu

Abbreviations used: aa, amino acid; Aβ, amyloid β peptide; APP, amyloid precursor protein; APPL, amyloid precursor protein-like; BiFC, bimolecular fluorescence complementation; CFP, cyan fluorescent protein; COS, SV40 transformed simian kidney fibroblast cell line; CTF, C-terminal fragment; DMEM, Dulbecco's modified Eagle's medium; E17, embryonic day 17; ER, endoplasmic reticulum; FACS, fluorescence-activated cell sorter; FBS, fetal bovine serum; GFP, green fluorescent protein; LIF, leukemia inhibitory factor; N2, Notch2; PBS, phosphate-buffered saline; NED, Notch extracellular domain; PCR, polymerase chain reaction; SDS–PAGE, sodium dodecyl sulfate – polyacrylamide gel electrophoresis; YC, YFP C-terminus; YFP, yellow fluorescent protein; YN, YFP N-terminus.

Sudhof 2004). Many functional models were proposed after the identification of protein binding partners. Some of these functions are attributed to the interaction of APP with extracellular proteins such as the heparan sulfate proteoglycans; others represent the interaction of APP with intracellular adaptor proteins such as Fe65, X11, APP-BP1 (Chow *et al*. 1996), PAK3 (McPhie *et al*. 2003) and kinesin [reviewed in De Strooper and Annaert (2000)]. Thus, it is possible that APP plays a role in various biological processes listed above by linking extracellular cues to intracellular signaling pathways via adaptor proteins acting as a cell surface receptor.

Recent accumulating evidence suggests a cross-talk between the processing and signaling of APP and the Notch family of receptors (Fassa *et al*. 2005; Fischer *et al*. 2005; Oh *et al*. 2005). Although the Notch signaling pathway has been most extensively studied in *Drosophila*, four mammalian homologs of Notch receptors have been characterized, Notch1–4. In parallel with the high sequence homology across species, Notch receptors share highly conserved signaling pathways of cell fate determination in the context of adulthood as well as development [reviewed in Gaiano and Fishell (2002); Selkoe and Kopan (2003)]. The activation of the Notch signaling pathway upon ligand binding involves sequential proteolytic processing of the receptor to generate the Notch intracellular domain (Schroeter *et al*. 1998), which, upon release from the plasma membrane, translocates to the nucleus. In the nucleus, the Notch intracellular domain binds with transcriptional regulators such as CBF1 to modulate transcription of target genes, i.e. *Hes*. The activation of the Notch signaling pathway is mediated by several ligands termed the DSL (delta and serrate/jagged in *Drosophila* and vertebrates, and Lag-2 in *Caenorhabditis elegans*), which themselves are single-pass transmembrane proteins predominantly from adjacent cells allowing for cell-to-cell communication. Although the canonical Notch signaling pathway was best characterized in *Drosophila*, knockout mouse models suggest its involvement in neural progenitor cell regulation and learning and memory [reviewed in Yoon and Gaiano (2005)].

In contrast, putative ligands for the extracellular portion of APP that affect its proteolytic processing and signaling have remained elusive. Evidence that APP can dimerize (Scheuermann *et al*. 2001) supports the idea that APP is a ligand-activated receptor. The first reported APP candidate ligand was F-spondin, a secreted signaling molecule implicated in neuronal development and repair (Ho and Sudhof 2004). Two recent studies described the interaction of APP with BRI2 protein, a type II membrane protein whose mutations cause a dementia with pathological features similar to Alzheimer's disease (Fotinopoulou *et al*. 2005; Matsuda *et al*. 2005). These studies found that BRI2 modulates the proteolytic processing of APP and inhibits Aβ production.

We previously initiated a search for molecules that bind to plasma membrane APP by employing a membrane-impermeable cross linker to immobilize proteins that bind to APP at the cell surface. We reported for the first time the identification of Notch2 (N2) as an APP binding partner, and we provided evidence that both N2 and its close homolog, Notch1 (N1), can be co-immunoprecipitated with APP (Oh *et al*. 2005). Two other groups reported the interaction of APP with Notch1 (Fassa *et al*. 2005; Fischer *et al*. 2005).

To visualize protein–protein interactions in living cells, Hu and colleagues recently described a technique termed bimolecular fluorescence complementation (BiFC) (Hu *et al*. 2002; Hu and Kerppola 2003). The BiFC approach is based on the formation of a fluorescent complex by fragments of the enhanced yellow fluorescent protein (YFP) brought together by the association of two interacting partners fused to the fragments. The advantages of BiFC analysis include: (i) the subcellular localization of protein interactions under conditions that closely reflect the normal physiological environment; (ii) BiFC fluorescence signals are easily detected by a fluorescence microscope equipped with either FITC, green fluorescent protein (GFP) or YFP filters compared with fluorescence resonance energy transfer, which requires either irreversible photo-bleaching or fluorescence lifetime imaging using instrumentation that is not widely available; (iii) the large number of GFP variants with distinct spectral characteristics provide the potential for parallel analysis of multiple protein interactions in the same cell.

In the present study, we utilized BiFC analysis to visualize the subcellular localization of the complexes formed by APP homodimers and APP/Notch heterodimers in living cells. We fused the N-terminal and C-terminal fragments of YFP to APP, N2, and a C-terminally truncated form of N2. When expressed in SV40 transformed simian kidney fibroblast cell line (COS) cells, these tagged proteins alone did not produce a fluorescent signal. The APP homodimer produced a weak fluorescent signal. Expression of either full-length N2 or its truncated form did not produce a visible fluorescent signal, suggesting that N2 receptors do not form homodimers. The strongest fluorescent signal was obtained by co-expression of the C-terminus of YFP fragment fused to APP and the N-terminus of YFP fragment fused to the truncated form of N2. The heterodimer formed by APP and the truncated form of N2 localized to the plasma membrane, endoplasmic reticulum (ER), Golgi and other intracellular vesicles. Fine adjustment of the linker region between APP and the C-terminus of YFP enhanced the fluorescence intensity of BiFC.

Materials and methods

Preparation of embryonic day 17 (E17) rat brain momogenate and co-immunoprecipitation

Pieces of E17 rat brain were weighed (0.5 g) and solubilized in 2.5 mL of the homogenation buffer [1% Triton X-100, 1 mM EDTA,

1 mM EGTA, 1 μg/mL aprotinin, 0.7 μg/mL pepstatin, 1 μg/mL leupeptin, 1 mM pefabloc, and 20 μM E-64 in 1 × phosphate-buffered saline (PBS)]. Homogenization was carried out with a Teflon-coated pestle (10 strokes), and the homogenate was passed through a 20-gauge needle (10 times). The brain homogenate was incubated on ice for 30 min and centrifuged at 16,000 ***g***. for 10 min at 4°C. The resulting supernatant was transferred to new eppendorf tubes and protein concentrations were measured using the Micro-BCA Protein Assay Reagent Kit (Pierce, Rockford, IL, USA) according to the manufacturer's instructions.

Brain homogenate containing 1 mg of total protein was pre-cleared using Protein G-Sepharose beads (Amersham Biosciences, Piscataway, NJ, USA) for 2 h at 4°C and immunoprecipitated overnight using monoclonal mouse APP N-terminal antibody 22C11 (Chemicon, Temecula, CA, USA). The antibody-bound complexes were isolated by incubation with Protein G sepharose beads for 2 h and washed three times using the homogenization buffer with 0.5% Triton X-100. The protein complexes were eluted in 5 × Laemmli sample buffer and analyzed by sodium dodecyl sulfate – polyacrylamide gel electrophoresis (SDS–PAGE) followed by Western blot with a polyclonal Notch1 antibody directed to the C-terminus of Notch1 (Nofziger *et al.* 1999).

Plasmid construction

The preparation of the APP YFP and N2 YFP constructs was described previously (Oh *et al.* 2005). To construct the N2C50 YFP plasmid, a *Sal*I site was introduced into the N2 YFP plasmid using QuickChange Site-Directed mutagenesis kit (Stratagene, La Jolla, CA, USA) with the following sense and antisense primers: 5′-CTCAGAAGCTAACCTGTCGACTACTGGAACAAGTGAA-3′ and 5′-TTCACTTGTTCCAGTAGTCGACAGGTTAGCTTCT-GAG-3′. The mutated N2 YFP plasmid with a *Sal*I site 50 amino acids (aa) downstream of the transmembrane domain of N2 cDNA sequence was digested with *Sal*I, which removed the N2 cDNA sequence encoding amino acid residues 1749–2471, and self-ligated. The resulting N2C50 YFP construct was confirmed by DNA sequencing.

The sequences encoding amino acid residues 1–154, 155–238, 1–172, and 173–238 of enhanced YFP, and cyan fluorescent protein (CFP) (Clontech, Mountain View, CA, USA) were fused downstream of sequences encoding either full-length APP, full-length N2 or N2C50 using linker sequences encoding STVPRARDPPVAT. The chimeric coding regions were cloned into the pcDNA1 mammalian expression vector (Invitrogen, Carlsbad, CA, USA). To construct the N2ΔEC50 YFP N-terminus (YN) plasmid, the following primers were used in a standard PCR reaction with pfu polymerase (Stratagene, La Jolla, CA, USA) using N2C50 YN plasmid as template: 5′-GTCAGTGAATCCCTGACTCC-3′ and 5′-ACACTGCAATGCA-TGCGCGGG-3′. The PCR product containing the cDNA and the pcDNA1 vector was isolated and self-ligated. The resulting N2ΔEC50 YN construct was confirmed by DNA sequencing. The plasmid encoding the ER marker, P450 2C2 CFP, was kindly provided by Dr Elzbieta Skorupa (UIUC, Urbana, IL, USA) (Szczesna-Skorupa *et al.* 2003). The plasmid encoding the Golgi marker, the 81 N-terminal amino acids of human 1,4-galactosyltransferase/DsRed2, was kindly provided by Dr Nikolaj Klocker (University of Freiburg, Germany) (Stockklausner and Klocker 2003).

SDS–PAGE, Western blotting and antibodies

Protein concentrations were measured using the Micro BCA Protein Assay Reagent Kit (Pierce, Rockford, IL, USA) according to the manufacturer's protocol. For SDS–PAGE, cell lysates containing 20 μg of total protein were boiled for 5 min and loaded on 4–20% pre-cast Tris-HCl gels (Bio-Rad Laboratories, Hercules, CA, USA). Proteins were transferred to nitrocellulose membranes (Millipore Corporation, Bedford, MA, USA). All antibodies were diluted in TBST [50 mM Tris, pH 8.0, 150 mM NaCl and 0.1% (v/v) Tween 20] containing 5% (w/v) non-fat dry milk (Carnation, Glendale, CA, USA). Secondary antibodies were horseradish peroxidase-conjugated goat anti-mouse or anti-rabbit (Kirkegaard & Perry Laboratories, Gaithersburg, MD, USA). Enhanced chemiluminescence was detected using SuperSignal® West Pico Chemiluminescent Substrate (Pierce, Rockford, IL, USA). Auto-radiography was carried out using Kodak Scientific Imaging Film X-OMAT™ AR (Eastman Kodak, Rochester, NY, USA).

The primary antibodies used were anti-Aβ monoclonal antibody 6E10 (Senetek, Napa, CA, USA), C8, a polyclonal antibody against the C-terminus of APP, a gift from D. Selkoe (Selkoe *et al.* 1988) and anti N-terminus of N2 rabbit polyclonal antibody (Abcam, Cambridge, MA, USA).

Imaging of fluorescence in living cells

COS-7 cells were maintained in Dulbecco's modified Eagle's medium supplemented with 10% fetal bovine serum and antibiotics at 37°C and 5% CO_2. Cells grown on a Laboratory-Tek II eight-chambered coverglass (Nalge Nunc International, Rochester, NY, USA) were co-transfected with 0.4 μg of the expression vectors indicated in each experiment using Lipofectamine Plus reagent (Invitrogen). The same amount of DNA was used for each co-transfection. For Mock and single plasmid transfection, 0.4 μg of pcDNAI empty vector was added. Twenty-four to forty-eight hours after transfection, cells were washed twice with PBS and the fluorescence was observed in living cells in PBS using a Zeiss Axiovert 200M microscope with YFP, CFP and rhodamine filters.

Flow cytometry

Forty-eight hours after transfection using 1 μg of each plasmid, COS-7 cells plated on six-well plates were washed with PBS, scraped and suspended in 1 mL PBS. The flow cytometric analyses of the single-cell suspensions were performed using a fluorescence-activated cell sorter (FACS; FACScan; BD Biosciences, San Jose, CA, USA) equipped with an argon laser emitting at 488 nm. Analysis was restricted to live cells by gating cells that exhibited forward and side-scatter features typical of live cells. Results from 10 000 cells were analyzed using CellQuest software (BD Biosciences) and the results were plotted as a distribution of cells versus YFP fluorescence in arbitrary units. The percentage and average fluorescent intensity of cells above the indicated threshold were shown in the figures.

Results

APP interacts with Notch1 in embryonic rat brain tissue

In the previous study, we identified Notch proteins as APP binding partners by mass spectrometry analysis of APP

complexes immunopurified from E18 neurons over-expressing APP751 (Oh *et al*. 2005). We further confirmed the interactions using co-expression of APP and N1 or N2 in mammalian cells, and co-immunoprecipitation of APP with Notch antibodies (Oh *et al*. 2005). To demonstrate that these interactions also occur under physiologic conditions and are not the result of over-expression artifacts, here we confirm the endogenous interaction of APP with Notch1 in E17 rat brain tissue extracted in 1% Triton X-100. Figure 1 shows that N1 was co-immunoprecipitated by the anti-APP antibody 22C11. A full-length N1 band was clearly detected (Fig. 1, lane 3), which was absent in the negative control immunoprecipitated with normal mouse IgG (Fig. 1, lane 4). The transiently expressed N1 in COS-7 cells and the lysate from E17 rat brain were used as positive controls (Fig. 1, lanes 1 and 2). The anti-N1 antibody used in this experiment recognized two strong bands in addition to full-length N1, which did not co-immunoprecipitated with APP (Fig. 1, lane 2 and 3), suggesting they were either non-specific bands or N1 fragments that do not interact with APP. Using the available antibodies to N2, we were not able to detect N2 protein in E17 rat brain. This could be because of the low level of N2 expression in E17 rat brain or the inability of the available N2 antibodies to recognize rat N2.

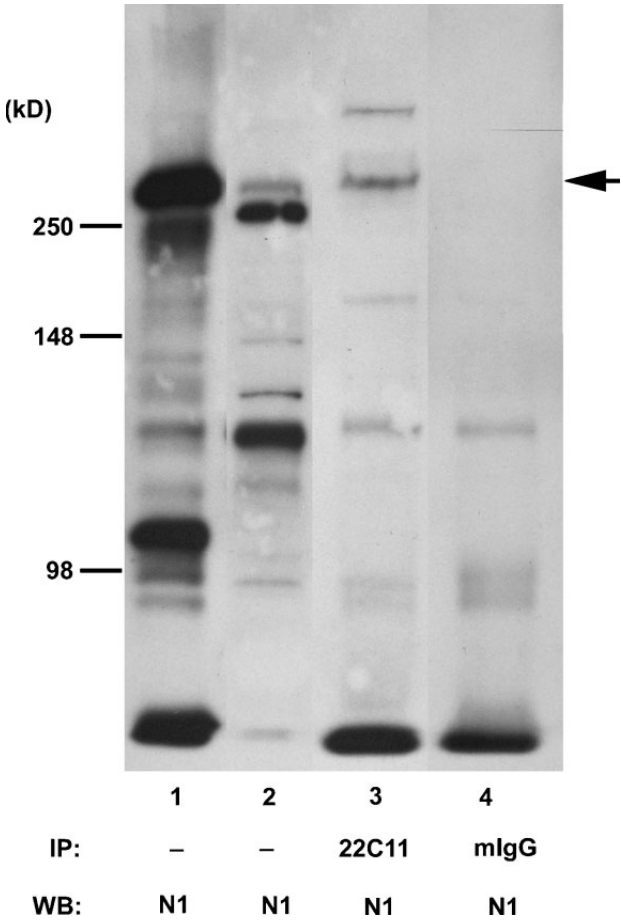

Fig. 1 Endogenous interaction of Notch1 and APP in E17 rat brain tissue. The cell lysate from COS-7 cells transiently expressing Notch1 was used as control in lane 1. The E17 rat brain tissue was homogenized in a lysis buffer containing 1% Triton X-100. The lysates containing ~10 μg of total protein were analyzed by SDS–PAGE and Western blot using pAb Notch1 C-term antibody to confirm the expression of Notch1 protein (lane 2). About 90% of protein in the homogenate (~2 mg) was incubated with anti-APP mAb 22C11 (lane 3) or normal mouse IgG (lane 4) as a control, and the antibody-bound proteins were precipitated with Protein G agarose. The isolated complexes were eluted with Laemmli samples buffer and analyzed by SDS–PAGE followed by Western blot with pAb Notch1 C-term antibody (IP, immunoprecipitation; 22C11, anti-APP mAb 22C11; N1, Notch1 C-term pAb; mIgG: normal mouse IgG; WB, Western blot). The arrow indicates full-length Notch1 protein.

BiFC analysis of APP/N2 heterodimeric interactions in living cells

BiFC assay provides the potential for direct visualization of protein interactions in living cells (Hu *et al*. 2002; Hu and Kerppola 2003). To investigate interactions between APP and the N2 protein in live cells, we co-transfected expression vectors encoding the N-terminal 1–154 aa and C-terminal 155–238 aa of YFP fragments fused to APP, full-length N2, and a C-terminally truncated form of N2 in several configurations (Figs 2a and b). We chose YFP because the fluorescence signal is easily detected by fluorescence microscopy equipped with FITC, GFP or YFP filters. The rationale behind using a C-terminally truncated N2 that contained only 50 aa (N2C50) of the cytosolic domain was to increase the chances for interaction between the two YFP fragments fused at the C-termini of APP and Notch, as the cytosolic domain of the N2 molecule is 773 aa long and is much longer than the APP cytosolic domain, which contains only 50 aa residues (Fig. 2b).

To demonstrate that APP and N2 constructs used in this work were expressed and processed normally, we transfected COS-7 cells with these two constructs and performed Western blotting using various antibodies to APP and N2. Using anti-APP mAb 6E10 and an anti-GFP antibody, we were able to detect APP YN and APP YFP C-terminus (YC), which were larger than APP because of tagging with the YFP fragment (Fig. 2e indicated by asterisks). We detected CTFs of APP with the C8 antibody (Fig. 2e, arrowhead 1), and the equivalent band of APP YC (CTF YC) using the anti-GFP antibody (Fig. 2e, arrowhead 2). Unfortunately, because the CTF YN band was the same size as that of a non-specific band, we were not able to detect CTFs clearly from this experiment (Fig. 2e, arrowhead 3). As GFP variants and myc tagged proteins were used in many other studies, the tagged APP proteins appeared to be functional and processed normally (Kinoshita *et al*. 2001, 2003; Oh *et al*. 2005). Our result suggested that APP tagged with YN and YC were expressed with the expected size and processed normally, at

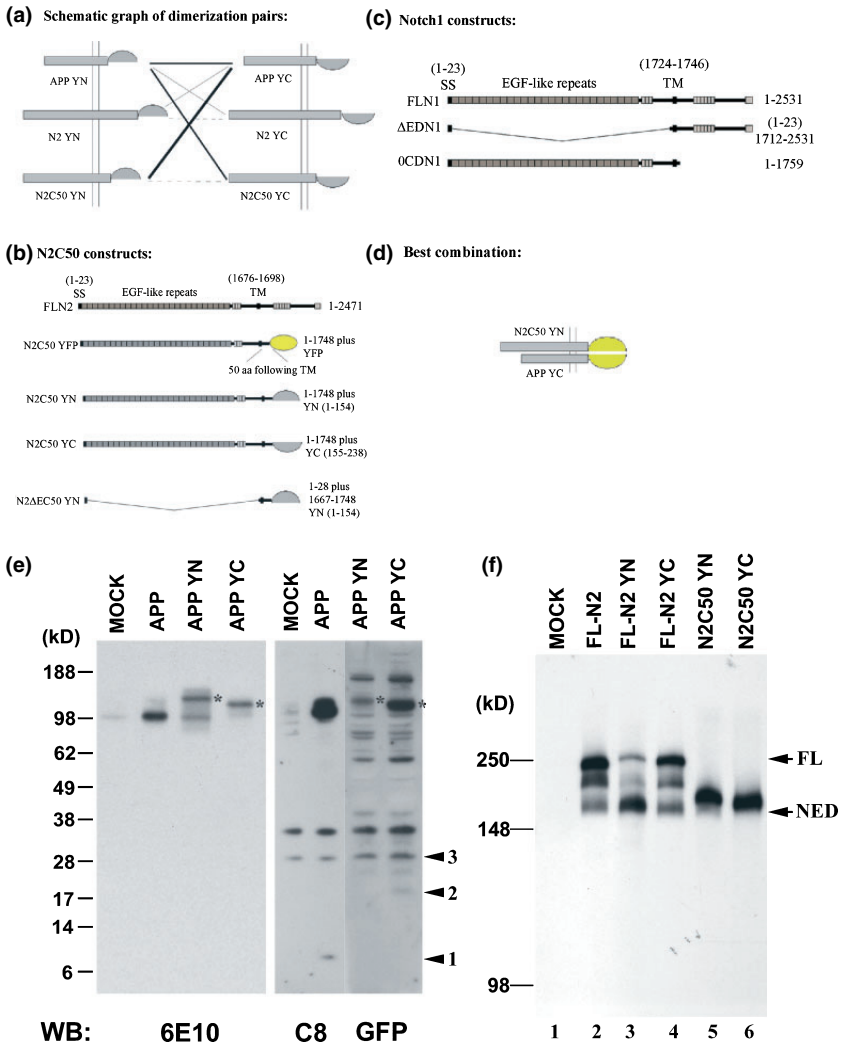

Fig. 2 The schematic diagram of dimerization pairs used in the BiFC analysis and the expression and processing of APP and Notch constructs. (a) Scheme of the protein pairs used. The thickness of the lines represents the intensity of the BiFC signal according to the fluorescent intensity obtained from the 'Histogram' analysis of each image normalized to cell autofluorescence using Openlab software (Improvision, Lexington, MA, USA). Note that the strongest BiFC signal from YFP fragments was obtained with co-transfection of N2C50 YN and APP YC. The combination of APP YN/APP YC and APP YN/N2C50 YC produced a somewhat weaker fluorescent signal, and the heterodimers of APP and full-length N2 produced a very weak BiFC signal. The dashed lines represent no detectable BiFC fluorescent signals for Notch homodimers. (b) Diagram of full-length N2 (FLN2) and N2C50 constructs fused to full-length YFP or N-terminal or C-terminal fragments of YFP. (c) Diagram of Notch1 constructs used in previous APP/Notch1 interaction experiments described in Oh *et al.* (2005). All three Notch1 constructs can be co-immunoprecipitated with APP. (d) Diagram of the combination that produces the strongest BiFC signal. (e) Western blot analysis of APP constructs used in the BiFC study. COS-7 cells transfected with the APP constructs indicated were lysed 48 h after transfection. The lysates were analyzed by SDS–PAGE and Western blotting with anti-APP mAb 6E10, pAb C8 or polyclonal anti-GFP antibody (Molecular Probes, Eugene, OR, USA). Asterisks indicate APP with either YN or YC-tag, which are larger than APP in molecular weight (18.8 kDa for YN and 10.9 kDa for YC). Arrowhead 1 indicates CTF from wild-type APP processing, arrowhead 2 indicates CTF with YC-tag (about 20 kDa), and arrowhead 3 indicates the theoretical position of CTF with YN-tag (about 28 kDa). (f) Western blot analysis of Notch2 constructs used in BiFC study. COS-7 cells transfected with Notch2 constructs indicated were lysed 48 h after transfection. The lysates were analyzed by SDS–PAGE and Western blotting with anti-Notch2 N-term polyclonal antibody. FL, full-length Notch2 constructs; NED, Notch2 extracellular domain.

least for APP YC. Figure 2(f) shows the transient expression of N2 constructs in COS-7 cells. We detect that the full-length proteins FL-N2 YN and FL-N2 YC migrate at the expected size, and are processed similarly to untagged FL-N2 (Fig. 2f, lanes 2–4). Although FL-N2 YN produced more Notch extracellular domain (NED), the pattern of processing was similar to FL-N2 (Fig. 2f, compare lanes 2 and 3). The NED band was clearly detected in the N2C50 YN construct

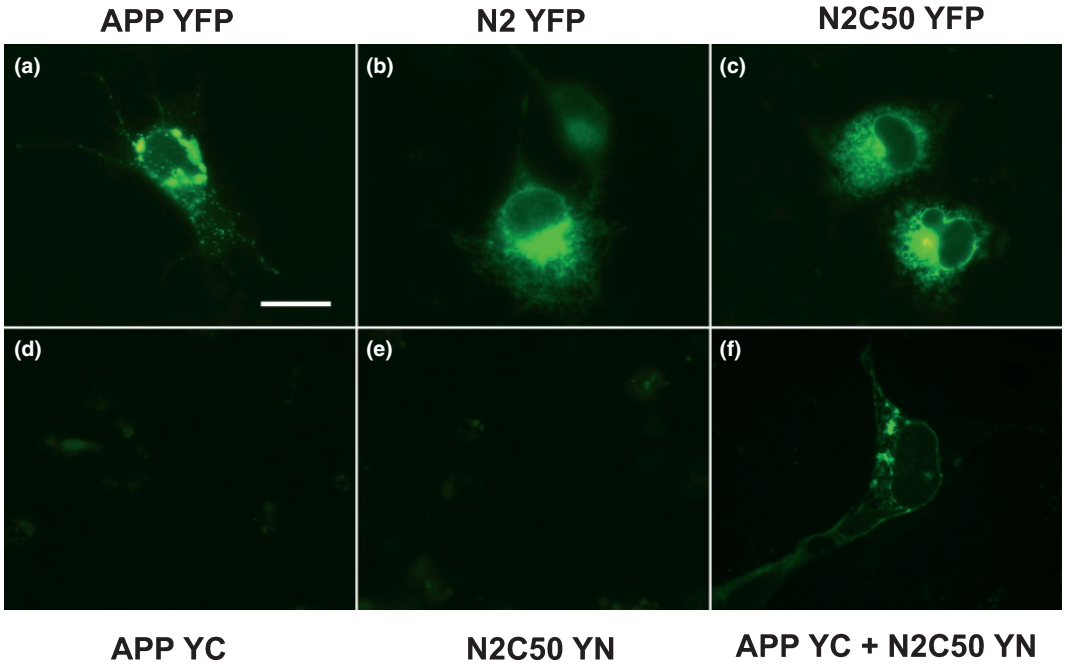

Fig. 3 Fluorescence imaging of APP and Notch proteins and their interaction in living COS-7 cells using BiFC analysis. (a–c) APP YFP, N2 YFP, and N2C50 YFP positive controls. (d, e), APP YC and N2C50 YN expressed alone as negative controls showing cell autofluorescence with no detectable BiFC signal. (f) Fluorescence image of cells

(Fig. 2f, lane 5), suggesting normal processing for this construct as well. The size of N2C50 YC was very close to the NED band, therefore it was difficult to detect the doublet (Fig. 2f, lane 6). Our results suggest that the N2 constructs used in this study are expressed and processed normally.

In the previous study, a C-terminally truncated form of N1 (Figs 2c, 0CDN1) interacted even more strongly with APP than the full length N1 (1–1759 aa) (Fotinopoulou *et al*. 2005; Oh *et al*. 2005). We therefore predicted that N2C50 would interact with APP as well. When expressed in COS-7 cells, any of these proteins alone failed to produce a fluorescent signal (Figs 3d and e). Indeed, as expected, the strongest fluorescent signal was obtained with co-expression of the C-terminus of YFP fragment fused to APP and the N-terminus of YFP fragment fused to the truncated form of N2. We were able to detect a fluorescent signal 24 h after transfection (Figs 2d and 3f). As positive controls, we transfected APP, N2 and N2C50 tagged at their C-termini with the full-length YFP protein into COS-7 cells and observed live cells under fluorescence microscopy (Figs 3a–c). Cells expressing APP YFP or N2 YFP showed the typical pattern of the cell surface proteins, localizing to the ER, Golgi, intracellular vesicles and the cell surface (Figs 3a and b). The expression pattern of N2C50 YFP was identical to that of full-length N2 YFP (Fig. 3c). When co-expressed in the same cells, the heterodimers formed by APP YC and N2C50 YN localized to plasma membrane, intracellular vesicles, and other unidentified subcellular compartments (Fig. 3f).

A comparison of the pattern of fluorescence between either APP YFP or N2 YFP alone with that of the APP YC/N2 YN heterodimer revealed that the fluorescent signal produced by APP YFP or N2 YFP was considerably stronger than that produced by the APP YC/N2C50 YN heterodimer (Figs 3a–c and f), suggesting that only a subset of APP molecules form heterodimers with N2 molecules in the cells or that the fluorescence complementation in the heterodimer is not as perfect as it is in the intact YFP parent molecule. Co-expression of APP YC and N2C50 YN (Figs 4a and b) yielded a strong fluorescent signal 48 h after transfection. Over-expressed proteins commonly leak into domains that do not normally contain the protein in question and thus lead to non-physiologic interactions. To demonstrate that APP and N2C50 interaction occurs even when cells express only modest levels of these proteins, we selected cells expressing different levels of APP and N2C50 (Fig. 4b). Cells with barely detectable levels of BiFC signal exhibited a similar subcellular distribution pattern as those with strong BiFC signals (Fig. 4b). Interestingly, the fluorescent signal from co-expression of APP YN and N2C50 YC was not as strong as that of the APP YC/N2C50 YN pair (Fig. 2a and Fig. 4c compared with Figs 4a and b), likely because the distance and orientation of the two YFP fragments with respect to each other resulted in weaker fluorescence. The fluorescent signal produced by the interaction of APP with full-length N2 was very weak compared with that obtained with the truncated N2 molecule (Fig. 4d), probably as a result of the large C-terminal cytosolic domain of the N2 molecule

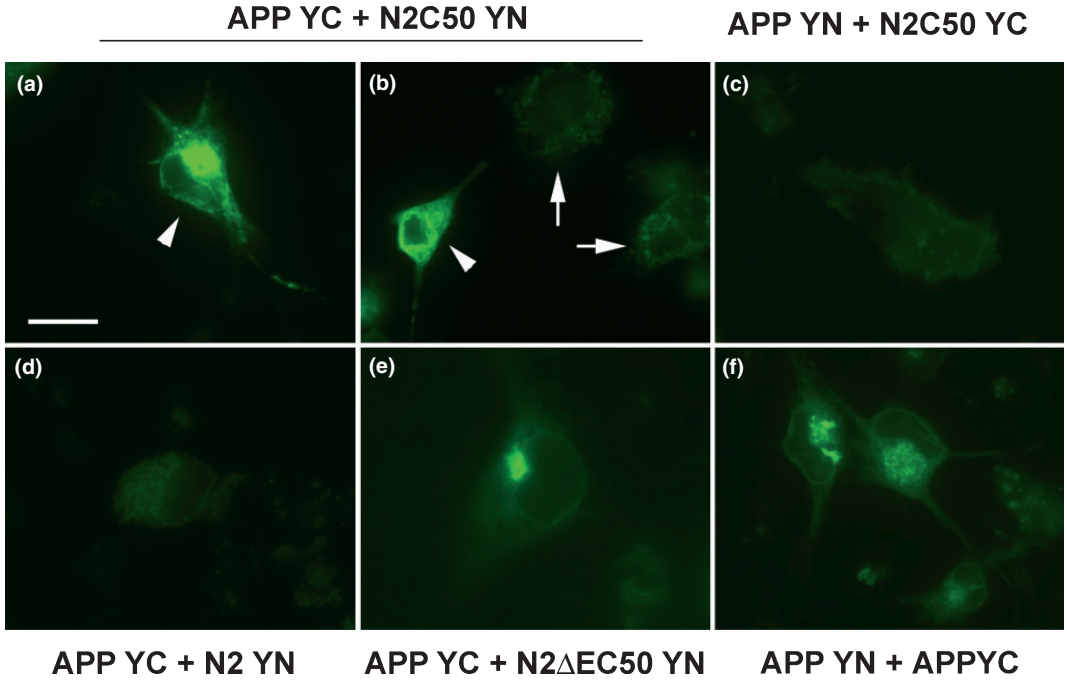

Fig. 4 BiFC analysis of APP and Notch constructs in living cells acquired 48 h after transfection. Fluorescence images of COS-7 cells co-expressing APP YC/N2C50 YN (a, b), APP YN/N2C50 YC (c), APP YC/N2 YN (d), APP YC/N2ΔEC50 YN (e), or APP YN/APP YC homodimers (f). Two images were selected (a, b) to show cells with different level of protein expression (arrows, low level; arrowheads, high level), but similar pattern of subcellular distribution.

relative to that of APP. Another explanation for the reciprocal constructs not producing similar BiFC signals is that different YN or YC-tags on APP or N2C50/N2 could interfere with the binding of these two molecules. Fortunately, we were able to find the optimal tagging combination for the APP/N2C50 interaction (Fig. 2d).

The subcellular distribution pattern of APP homodimers and APP/N2C50 heterodimers is somewhat different. The APP homodimers appear to localize around the nucleus in a heavy perinuclear dot structure (Fig. 4f). In contrast, the APP/N2C50 heterodimers show a more even distribution pattern within the cells, more consistent with localization in the ER, Golgi, as well as with the plasma membrane (Figs 4a and b). These results confirm our previous proteomic and biochemical findings of APP and N2 interactions, and provide a more detailed APP/N2 and APP/N2C50 interaction pattern within the cells which is superior to that obtained with the previous indirect immunofluorescence method (Oh *et al*. 2005).

Minimum requirement of Notch domains for the APP/Notch interaction

In the previous study, we found that the N1 protein can interact with APP even when most of the C-terminus cytosolic domain was truncated (1–1759 aa of N1, with only 13 aa left following the putative TMD, see Fig. 2c, 0CDN1 construct) (Oh *et al*. 2005). Another transmembrane construct consisting of the 1–23 aa signal sequence followed by aa 1712–2351 of N1 also interacted with APP, suggesting that aa 1712–1759, which include the TM region (aa 1724–1746) of the N1 protein contains an APP-interacting motif [see Fig. 2c and Oh *et al*. (2005)]. To determine whether or not the APP interacting motif resided within a similar region of the N2 protein, we constructed a N2ΔEC50 YN plasmid with the N-terminal 28-aa signal sequence of N2 followed by aa 1667–1748 of N2 fused to YN (1–154) (Fig. 2b). Co-transfection of APP YC and N2ΔEC50 YN revealed a pattern of subcellular distribution similar to that seen with the APP YC and N2C50 YN heterodimer; however, the fluorescence intensity was less than that of the APP YC/N2C50 YN pair (Fig. 4e compared with Figs 4a and b). This result suggests that there is an APP binding motif within aa 1667–1748 of the N2 protein, most likely within the TM domain of N2 protein (with a possible contribution from the extracellular 9 aa and the intracellular 13 aa of the juxtamembrane region).

BiFC analysis of APP and N2 homodimeric interactions in living cells

It has been reported that APP forms homodimers; and the data presented by Scheuermann and colleagues suggested that Aβ production might be positively regulated by APP dimerization (Scheuermann *et al*. 2001). To confirm the occurrence of APP dimerization in our BiFC system, we co-transfected APP YN and APP YC into COS-7 cells and examined the cells by fluorescence microscopy. The APP

homodimers produced a weaker fluorescent signal 48 h after transfection than that observed for the APP/N2C50 heterodimers (Fig. 4f). Thus, APP dimerization served as a positive control for our BiFC studies. In contrast, expression of the YN and YC tagged full-length N2 or its truncated form did not produce a visible fluorescent signal, suggesting that N2 receptors do not form homodimers (Fig. 2a, fluorescence image not shown). These results were consistent with recent findings by Voojis *et al*. that, although the Notch epidermal growth factor repeats can promote dimer formation, most surface Notch molecules in mammalian cells are monomeric (Vooijs *et al*. 2004). Thus, the lack of dimerization of N2 receptor proteins served as a negative control in our BiFC analysis.

Fine adjustment of the linker region between APP and YC fragment increases the number of cells exhibiting fluorescent signals

The length of the linker region and the orientation of the two YFP fragments with respect to each other help determine the intensity and kinetics of the fluorescent signal. From a data set of 638 multidomain protein chains, George and Heringa (2002) found 1280 linkers, totaling 12 776 residues. Linkers were found to have an average length of 10.0 ± 5.8 residues. Furthermore, it has been reported that Thr, Ser, Pro, Asp, Gly, Lys, Gln, Asn and Ala (in the order of decreasing preference) are the preferred residues in linkers (Argos 1990; Chen and Kemper 1996). The linker sequence used in this study was STVPRARDPPVAT, a total of 13 aa residues containing most of the preferred residues found in linkers. As it is well known that APP forms homodimers in cells, we were surprised by the result that the APP YN/APP YC pair exhibited a much weaker fluorescence signal than did the APP/N2C50 heterodimers (Figs 2a, 3 and 4). To fine tune the fluorescence signal produced by APP YN and APP YC homodimers, the linker region between APP and the YC fragment was reduced from 13 aa residues to either 12, 11, or 10 aa residues (Fig. 5a), and the cells co-expressing APP YN with either APP YC, APP Δ1YC, Δ2YC, and Δ3YC were examined under fluorescence microscopy (Fig. 5b). All pairs of the APP homodimers exhibited a similar pattern of distribution in cells, and exhibited very similar fluorescence signals (Fig. 5b). However, the number of cells exhibiting fluorescence signals was substantially increased when APP YN was co-transfected with APP Δ1YC, as quantified by FACS analysis (Fig. 6c).

In the case of the APP/N2C50 heterodimers, although we observed that a maximum number of cells exhibited fluorescence signals with the APP Δ1YC/N2C50 YN pair, the pattern of subcellular distribution was very similar among all pairs (Fig. 5b).

FACS analysis of the BiFC fluorescence signal

To quantify the BiFC fluorescence intensity, we used FACS analysis to determine the efficiency of fluorescence complementation in cells transfected with the various APP and Notch constructs. As shown in Fig. 6(a), cells transfected with the control APP YFP or N2 YFP exhibited a wide range of fluorescence values, with mean values of 126.52 and 297.57, respectively (arbitrary fluorescence units). The APP YFP and N2 YFP controls reflect our transfection efficiency, that should be close to the percentage of cells exhibiting higher fluorescence, which were 22.35 and 25.81%, respectively (Fig. 6a, table). N2C50 YFP exhibited a pattern similar to that of the APP YFP and N2 YFP controls (data not shown). Mock transfected cells, as well as cells transfected with either N2C50 YN or APP Δ1YC, produced no fluorescence signals other than the COS-7 cells autofluorescence (Figs 6a and b). When APP YC and N2C50 YN were co-transfected, we detected a second peak with a mean value of 14.05 ± 10.08 (Fig. 6a). The proportion of co-transfected cells showing BiFC was about 89% (19.9/22.35) or 77% (19.9/25.81) compared with the percentage of APP YFP and N2 YFP controls (Fig. 6a). The mean fluorescence intensity of this second peak was apparently much lower than the mean fluorescence intensity of the APP YFP control. This finding is consistent with our observations made using fluorescence microscopy, which revealed that the intensity of BiFC was 10–20 times lower than that of positive controls over-expressing full-length YFP.

The quantitative FACS study of the effects of fine adjustment of linker region is consistent with the fluorescence signals observed under the microscope. In the case of APP/N2C50 heterodimers, we observed maximum numbers of fluorescent

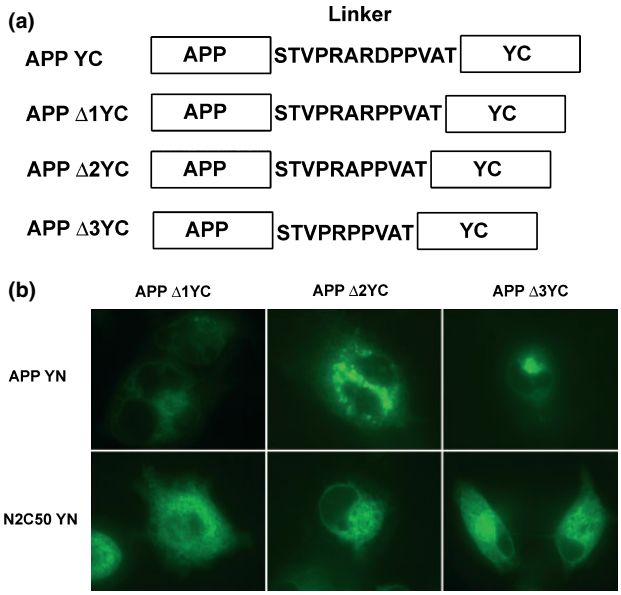

Fig. 5 Fine adjustment of the linker region between APP and YC fragment. (a) The amino acid sequences of the linker region between APP and YC fragment of APP YC, APP Δ1YC, APP Δ2YC, or APP Δ3YC. (b) BiFC analysis of COS-7 cells co-expressing the proteins indicated in each panel 48 h after transfection.

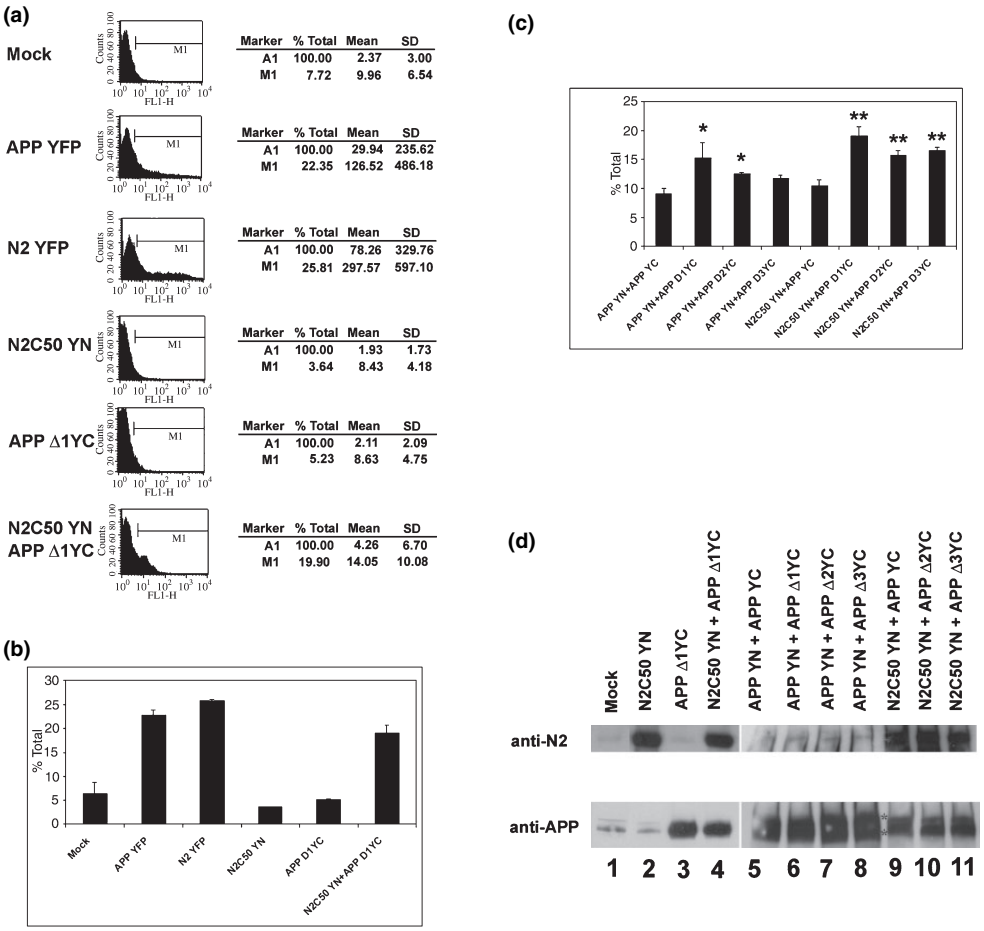

Fig. 6 Quantitation of BiFC by FACS analysis. (a) FACS analysis of COS-7 cells transfected with the indicated constructs. The M1 region was chosen to best estimate the percentage of cells exhibiting BiFC signal in co-transfection of N2C50 YN/APP Δ1YC. The percentage total, mean and standard deviation (SD) in each experiment are shown in the right panel. (b) The average of the percentage total in (a) from three independent transfections. Error bars represent SD of the average of percentage total ($n = 3$). The SD is calculated using the 'non-biased' or 'n-1' method. (c) FACS analysis of COS-7 cells co-transfected with the linker region variants shown in Fig. 5. Error bars represent SD of the average of percentage total ($n = 3$). Significant of results: *p-value of < 0.05 versus APP YN + APP YC; **p-value of < 0.01 versus N2C50 YN + APP YC. (d) Half of the cells transfected for FACS analysis were collected, lysed and analyzed by Western blotting with either anti-Notch2 extracellular domain polyclonal antibody or anti-APP 6E10 monoclonal antibody to ascertain equal transfection efficiency. Note that the intensity of the APP YN and APP YC doublets (asterisk) in APP homodimers were about the same (lower panel, lanes 5–8). The mature glycosylated forms of APP were detected in some of the lanes (lanes 1 and 2 endogeous APP from COS-7 cells, and lanes 4 and 9–11 higher bands).

cells with the APP Δ1YC and N2C50 YN pair (Fig. 6c). These data suggest that, by adjusting the length of the linker region, we were able to enhance the fluorescence signal produced by the two YFP fragments by 68% for the APP homodimer and by 84% for the APP/N2C50 heterodimer. The best combination of linkers in our case was 13 (YN) and 12 (YC) for both the APP homodimers, and the APP/N2C50 heterodimers. By manipulating the linker ratios, one can apply this technique to any study of protein–protein interactions.

To ensure that each transfection produced a similar level of protein expression, half of the cells transfected for FACS analysis were collected, lysed and analyzed by Western blotting with either anti-Notch2 extracellular domain polyclonal antibody or anti-APP 6E10 monoclonal antibody (Fig. 6d). As expected, all the cells transfected with Notch2 variants expressed similar amounts of Notch2 protein (Fig. 6d, upper panel, lanes 2, 4, and 9–11). Cells transfected with APP variants also showed similar protein expression (Fig. 6d, lower panel, lanes 3, 4, and 9–11), and the intensity of bands of APP YN and APP YC variants was about the same (Fig. 6d, lower panel, lanes 5–8).

Co-localization of APP and Notch2 heterodimers with ER and Golgi markers

The APP/N2 heterodimers exhibited an even distribution pattern within the cells, consistent with an ER, Golgi and

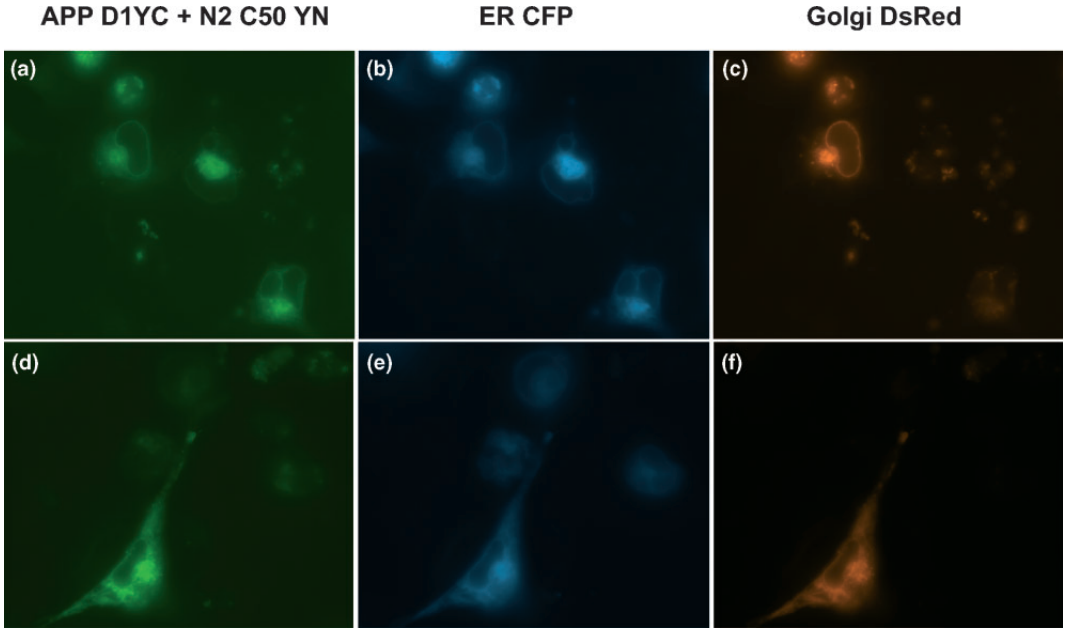

Fig. 7 Co-localization of APP and Notch heterodimers with ER and Golgi markers. Fluorescence images of COS-7 cells co-expressing APP Δ1YC/N2C50 YN together with P450 2C2/CFP (ER CFP) and 1,4-galactosyltransferase/DsRed2 (Golgi DsRed) markers in living cells acquired 48 h after transfection. Live cells were observed under the microscope with YFP (a, d), CFP (b, e) and rhodamine filters (c, f).

plasma membrane localization (Figs 4a–d, and 5b). To investigate the localization in more detail, we co-transfected COS-7 cells with ER CFP, and Golgi-DsRed markers, together with N2C50 YN/APP Δ1YC pairs. As shown in Fig. 7, the APP/N2C50 heterodimers co-localized with the ER and Golgi-markers.

Multicolor fluorescence complementation analysis

As BiFC analysis promises great potential for visualization of multi-protein interactions in the same cell, we sought to use different GFP variants fused to APP and Notch to observe homodimerization and heterodimerization in the same cell. We fused aa 1–173 of CFP to APP, and co-transfected APP CN173 with APP YC155 and N2C50 YN155. APP CN173/APP YC155 did not produce any detectable fluorescence. [Hu and colleagues obtained different results when studying Fos and Jun interactions. These researchers were able to detect BiFC with bJunCN173 and bFosYC155 (Hu and Kerppola 2003). One possible reason for this discrepancy could be the different length of the linker region used in their study.] We then constructed APP CN155 and co-transfected this plasmid with APP YC155 and N2C50 YN155. We were able to detect only a weak fluorescent signal using these combinations (data not shown). However, the fluorescent signal was so weak that it was usually bleached by the time we attempted to record the digital image. Further work is therefore necessary to visualize multiple-protein interactions simultaneously.

Discussion

In this study, we demonstrated endogenous APP/Notch1 interaction in E17 rat brain, suggesting the interaction was not likely because of over-expression artifacts. We visualized, for the first time, APP dimerization and APP/N2 heterodimerization in living cells using BiFC analysis. In contrast to APP, neither full-length N2, nor N2C50 formed homodimers. The homodimerization of APP exhibited a pattern of distribution in ER, Golgi, and other subcellular compartments, with no obvious cell surface localization pattern. The APP/N2C50 dimer, however, showed a considerably stronger fluorescent signal, and distributed to ER, Golgi, plasma membrane and possibly other unidentified intracellular compartments. A maximal fluorescence signal was obtained when the C-terminal half of YFP fused to APP was co-expressed with the N-terminal half of YFP fused to N2C50 that had the same length of cytosolic domain as APP. We were able to quantify the BiFC using FACS analysis, and we showed that about 20% of cells (77 or 89% of the transfected cells) co-expressing the APP YC/N2C50 YN pair exhibited fluorescence signals with an average fluorescence intensity approximately nine times weaker than that of the APP YFP control.

Recently, three groups have documented the interaction of APP and Notch proteins (Fassa *et al.* 2005; Fischer *et al.* 2005; Oh *et al.* 2005). All of the interactions observed, including this work using the BiFC technique, were detected only in transient expression systems over-expressing both

APP and Notch proteins. In order to ascertain that these interactions were not a result of over-expression artifacts, we co-immunoprecipitated APP with Notch1 from E17 rat brain homogenate, suggesting that endogenous APP and Notch1 also interact. Therefore, we strongly believe that the interaction is biologically relevant.

Implications of the APP dimerization

A comparison of the intensity and distribution pattern of APP YFP and APP homodimers (Figs 3a and 4f) revealed that APP YFP was distributed more widely than APP homodimers in ER and subcellular vesicles. We would like to emphasize that the fluorescence signal observed represents not only full-length APP YFP, including both monomers and dimers, but also C-terminal fragments of APP that contain YFP at their C-termini, and possibly also contain Aβ. In contrast, the images of the APP BiFC complex represent a subset of either full-length or C-terminal fragments of APP YN and APP YC dimers, but not APP monomers. It has been suggested that Aβ production can be positively regulated by APP dimerization because a single APP substitution at position 28 of Aβ (K624C) stabilized APP dimerization and increased Aβ production 6–8 fold. (Scheuermann *et al.* 2001). Thus, the BiFC positive APP may represent the pool of APP that has not yet been processed.

We are puzzled by the weak fluorescence signal exhibited by APP homodimerization. Although we were able to increase the number of cells producing a BiFC signal by shortening the length of the linker region, microscopic examination revealed that the fluorescence signal produced within each cell did not increase significantly (Fig. 5b). FACS analysis confirmed that, although some linkers yielded a greater number of fluorescent cells, the intensity of the fluorescence was very similar among all linker mutant pairs (Fig. 6). Like all other assay systems, BiFC analysis has its limitations: the fluorescent signal produced by complementation of the two halves of YFP fragments was not always strong enough to be detected by fluorescence microscopy. Judging from the images obtained, the fluorescence signal most likely gradually accumulated until it crossed a detectable threshold, which was at least above the level of COS-7 cell auto-fluorescence, in order to be considered a significant fluorescent signal quantifiable by FACS analysis. Fine-tuning of the linker region resulted in a greater number of cells exhibiting a detectable fluorescent signal, but did not increase the level of fluorescence in individual cells. The limiting factor may be the limited space available for the interacting proteins: in this case ER, Golgi and other compartments. Another explanation is that the BiFC signals did not have time to form in APP homodimers. APP turnover rate on the cell membrane is around 20–30 min (Weidemann *et al.* 1989), whereas the half-life of bimolecular fluorescent complex formation is nearly 50 min (Hu *et al.* 2002). If APP homodimerization facilitates Aβ production, then one would suspect that these dimers are very transient, leaving insufficient time for BiFC to produce a strong signal. Magliery *et al.* (2005) reported recently that the YN + YC fluorophore formation is irreversible, and, once it is formed, the protein–protein interaction is not required to maintain the reassembled YFP. Thus, theoretically, once the APP dimer is formed, the BiFC complex would continue to exhibit a fluorescent signal even after the processing of APP. However, the complex is likely also degraded in the compartments that process APP. A third possibility is that the two halves of the YFP fragments were too far away from each other to produce a strong BiFC signal. It was suggested that APP may dimerize via an N-terminal anti-parallel interaction between the E_2 domains, and that the distance between the C-terminal cytosolic domain would be around 60 Å (Wang and Ha 2004). Thus, the distance between the two C-terminal parts of APP within each dimer may be too far to produce a strong BiFC signal.

Implication of N2/APP heterodimerization

The strongest BiFC signal was obtained when APP YC and N2C50 YN were co-expressed. The pattern of distribution suggested that the interaction sites included ER, Golgi, cell membranes and some unidentified vesicles. These results were consistent with our previous indirect immunofluorescence data and biochemical analysis. As judged by the Western blot results, we were able to co-immunoprecipitate both the ER (immature) and Golgi (mature) forms of APP with the N2 antibody (Oh *et al.* 2005). The fact that we observed a strong BiFC signal under the microscope suggested that APP and N2C50 form a stable complex with a half-life that is longer than 50 min, the time required to produce a BiFC signal once the two halves bind to each other (Hu *et al.* 2002). This result implied that the binding did not result in the degradation of the APP/N2C50 complex, or at least not the BiFC complex. However, we do not know whether the processing of APP or N2C50 was affected, as they could be processed with the intracellular domain remaining intact.

In an *in vivo* model system, Loewer and colleagues used *Drosophila* to study the effects of over-expression of the mammalian APP, APLP1 and -2, and the fly amyloid precursor protein-like (APPL). They found that APP over-expression induced a reduction in Notch signaling. They suggested that the phenotypes observed are the consequence of putative cross-talk between the APP family and the Notch pathway, with Numb and Dab playing central roles as mediators (Loewer *et al.* 2004). In addition, a recent publication demonstrated cross-talk between Notch1 and APP signaling in Down's syndrome. Fischer and colleagues found that activation of Notch1 can *trans*-activate the APP target gene, *Kai1*, and vice versa (Fischer *et al.* 2005). The data presented here describing APP/Notch interactions favor the hypothesis that the APP/Notch complex prevents Notch processing/signaling, possibly through interfering with Notch

ligand binding. This possibility is currently under investigation.

The results from our previous biochemical studies suggested that there were two possible interaction sites with APP in the Notch molecule, one in the N-terminal extracellular domain and a second one near the TM domain (Oh *et al*. 2005). Following intracellular proteolytic processing of the full-length protein in Golgi, Notch is expressed at the cell surface as a heterodimeric receptor. Because both fragments of Notch contain APP interaction domains, we speculate that APP interacts with both parts of the Notch molecule. When co-expressing N2ΔEC50 YN and APP YC, we found that fewer cells exhibited a cell surface distribution pattern compared with cells expressing the N2C50 YN/APP YC pair (Figs 4a, b and e); moreover, the percentage of cells exhibiting fluorescence and the mean fluorescence values were both reduced by 33 and 29%, respectively, using FACS analysis. The loss of the fluorescent signal that is observed with the N2 construct lacking the extracellular domain supports our previous finding that APP interacts with the extracellular domain of N2 (Oh *et al*. 2005).

In our earlier study using chemical cross-linking, mass spectrometry, co-immunoprecipitation and indirect immunofluorescence to demonstrate the APP/Notch interaction, we were not able to rule out the involvement of a third adaptor molecule that could bring APP and Notch together. As APP and Notch are both γ-secretase substrates, the γ-secretase complex proteins (presenilin, nicastrin, pen2 and aph1) are potential candidates, together or alone, as bridge molecules. However, our results from the BiFC analysis favor a direct interaction, as, for this method to work, the two halves of the YFP fragments have to be brought very close together. At this time we cannot rule out other proteins that could participate in the APP/Notch interaction. Moreover, we do not know whether an intercellular (*trans*) or only a *cis* intracellular interaction exists between APP and Notch. By carefully designing the location and orientation of the YFP fragments in APP and Notch, it may be possible to visualize a *trans* interaction that would indicate cell-to-cell communication and signaling.

BiFC as a tool to study protein–protein interactions

Although the technique has been introduced only recently, there is already a multitude of studies of protein–protein interactions using BiFC analysis (Galarneau *et al*. 2002; Bracha-Drori *et al*. 2004; Grinberg *et al*. 2004; Hynes *et al*. 2004; Walter *et al*. 2004; Ozalp *et al*. 2005). We are confident that the fluorescent signals produced by our bimolecular complex are not false positive because (i) we were able to detect BiFC 24 h after transfection, (ii) not all of our combinations showed BiFC (the N2 and N2C50 dimers did not), and (iii) the patterns of the subcellular distribution were different among different combinations (e.g. APP dimers vs. APP/Notch heterodimers). This method is very promising for the visualization in the same living cell of multiple color interactions. So far, we were unable to produce a strong enough BiFC signal with fluorescent proteins other than those fused to YFP or its fragments. We are currently preparing constructs with different linkers, and using GFP variants to increase the BiFC signal. The BiFC analysis opens a new avenue to study protein–protein interactions in living cells and in the future it may be also possible to visualize intercellular interactions in living cells. Our present study in which we specifically visualized APP/Notch interactions could have diverse applications in understanding the roles of APP and Notch in development, normal aging and disease.

Acknowledgements

We thank G. Weinmaster for the Notch constructs and antibodies, D. J. Selkoe for the C8 antibodies, K. Kirsch for the use of the fluorescent microscope, and B. Kemper and E. Szczesna-Skorupa for helpful discussions. We also thank R. Neve, B. Wolozin, and L. Mucke for critical reading of the manuscript. This work was supported partly by NIH-NIA AG00001 and NIH-NIA AG00115.

References

Argos P. (1990) An investigation of oligopeptides linking domains in protein tertiary structures and possible candidates for general gene fusion. *J. Mol. Biol.* **211**, 943–958.

Ashley J., Packard M., Ataman B. and Budnik V. (2005) Fasciclin II signals new synapse formation through amyloid precursor protein and the scaffolding protein dX11/Mint. *J. Neurosci.* **25**, 5943–5955.

Bracha-Drori K., Shichrur K., Katz A., Oliva M., Angelovici R., Yalovsky S. and Ohad N. (2004) Detection of protein–protein interactions in plants using bimolecular fluorescence complementation. *Plant J.* **40**, 419–427.

Cao X. and Sudhof T. C. (2004) Dissection of amyloid-β precursor protein-dependent transcriptional transactivation. *J. Biol. Chem.* **279**, 24 601–24 611.

Chen C. D. and Kemper B. (1996) Different structural requirements at specific proline residue positions in the conserved proline-rich region of cytochrome P450 2C2. *J. Biol. Chem.* **271**, 28 607–28 611.

Chen Y., Liu W., McPhie D. L., Hassinger L. and Neve R. L. (2003) APP-BP1 mediates APP-induced apoptosis and DNA synthesis and is increased in Alzheimer's disease brain. *J. Cell Biol.* **163**, 27–33.

Chow N., Korenberg J. R., Chen X. N. and Neve R. L. (1996) APP-BP1, a novel protein that binds to the carboxyl-terminal region of the amyloid precursor protein. *J. Biol. Chem.* **271**, 11 339–11 346.

Combs C. K., Karlo J. C., Kao S. C. and Landreth G. E. (2001) β-Amyloid stimulation of microglia and monocytes results in TNFα-dependent expression of inducible nitric oxide synthase and neuronal apoptosis. *J. Neurosci.* **21**, 1179–1188.

De Strooper B. and Annaert W. (2000) Proteolytic processing and cell biological functions of the amyloid precursor protein. *J. Cell Sci.* **113**, 1857–1870.

Fassa A., Mehta P. and Efthimiopoulos S. (2005) Notch 1 interacts with the amyloid precursor protein in a Numb-independent manner. *J. Neurosci. Res.* **82**, 214–224.

Fischer D. F., van Dijk R., Sluijs J. A., Nair S. M., Racchi M., Levelt C. N., van Leeuwen F. W. and Hol E. M. (2005) Activation of the

Notch pathway in Down's syndrome: cross-talk of Notch and APP. *FASEB J.* **19**, 1451–1458.

Floden A. M., Li S. and Combs C. K. (2005) β-Amyloid-stimulated microglia induce neuron death via synergistic stimulation of tumor necrosis factor-α and NMDA receptors. *J. Neurosci.* **25**, 2566–2575.

Fotinopoulou A., Tsachaki M., Vlavaki M., Poulopoulos A., Rostagno A., Frangione B., Ghiso J. and Efthimiopoulos S. (2005) BRI2 interacts with amyloid precursor protein (APP) and regulates amyloid β (Aβ) production. *J. Biol. Chem.* **280**, 30 768–30 772.

Gaiano N. and Fishell G. (2002) The role of notch in promoting glial and neural stem cell fates. *Annu. Rev. Neurosci.* **25**, 471–490.

Galarneau A., Primeau M., Trudeau L. E. and Michnick S. W. (2002) β-Lactamase protein fragment complementation assays as *in vivo* and *in vitro* sensors of protein–protein interactions. *Nat. Biotechnol.* **20**, 619–622.

Gao Y. and Pimplikar S. W. (2001) The γ-secretase-cleaved C-terminal fragment of amyloid precursor protein mediates signaling to the nucleus. *Proc. Natl Acad. Sci. USA* **98**, 14 979–14 984.

George R. A. and Heringa J. (2002) An analysis of protein domain linkers: their classification and role in protein folding. *Protein Eng.* **15**, 871–879.

Grinberg A. V., Hu C. D. and Kerppola T. K. (2004) Visualization of Myc/Max/Mad family dimers and the competition for dimerization in living cells. *Mol. Cell Biol.* **24**, 4294–4308.

Herms J., Anliker B., Heber S., Ring S., Fuhrmann M., Kretzschmar H., Sisodia S. and Muller U. (2004) Cortical dysplasia resembling human type 2 lissencephaly in mice lacking all three APP family members. *EMBO J.* **23**, 4106–4115.

Ho A. and Sudhof T. C. (2004) Binding of F-spondin to amyloid-β precursor protein: a candidate amyloid-β precursor protein ligand that modulates amyloid-β precursor protein cleavage. *Proc. Natl Acad. Sci. USA* **101**, 2548–2553.

Hu C. D. and Kerppola T. K. (2003) Simultaneous visualization of multiple protein interactions in living cells using multicolor fluorescence complementation analysis. *Nat. Biotechnol.* **21**, 539–545.

Hu C. D., Chinenov Y. and Kerppola T. K. (2002) Visualization of interactions among bZIP and Rel family proteins in living cells using bimolecular fluorescence complementation. *Mol. Cell* **9**, 789–798.

Hynes T. R., Tang L., Mervine S. M., Sabo J. L., Yost E. A., Devreotes P. N. and Berlot C. H. (2004) Visualization of G protein βγ dimers using bimolecular fluorescence complementation demonstrates roles for both β and γ in subcellular targeting. *J. Biol. Chem.* **279**, 30 279–30 286.

Kamal A., Stokin G. B., Yang Z., Xia C. H. and Goldstein L. S. (2000) Axonal transport of amyloid precursor protein is mediated by direct binding to the kinesin light chain subunit of kinesin-I. *Neuron* **28**, 449–459.

Kimberly W. T., Zheng J. B., Guenette S. Y. and Selkoe D. J. (2001) The intracellular domain of the β-amyloid precursor protein is stabilized by Fe65 and translocates to the nucleus in a notch-like manner. *J. Biol. Chem.* **276**, 40 288–40 292.

Kinoshita A., Whelan C. M., Smith C. J., Mikhailenko I., Rebeck G. W., Strickland D. K. and Hyman B. T. (2001) Demonstration by fluorescence resonance energy transfer of two sites of interaction between the low-density lipoprotein receptor-related protein and the amyloid precursor protein: role of the intracellular adapter protein Fe65. *J. Neurosci.* **21**, 8354–8361.

Kinoshita A., Fukumoto H., Shah T., Whelan C. M., Irizarry M. C. and Hyman B. T. (2003) Demonstration by FRET of BACE interaction with the amyloid precursor protein at the cell surface and in early endosomes. *J. Cell Sci.* **116**, 3339–3346.

Koo E. H., Sisodia S. S., Archer D. R., Martin L. J., Weidemann A., Beyreuther K., Fischer P., Masters C. L. and Price D. L. (1990) Precursor of amyloid protein in Alzheimer disease undergoes fast anterograde axonal transport. *Proc. Natl Acad. Sci. USA* **87**, 1561–1565.

Li X., Burklen T., Yuan X., Schlattner U., Desiderio D. M., Wallimann T. and Homayouni R. (2005) Stabilization of ubiquitous mitochondrial creatine kinase preprotein by APP family proteins. *Mol. Cell Neurosci.* (in print).

Loewer A., Soba P., Beyreuther K., Paro R. and Merdes G. (2004) Cell-type-specific processing of the amyloid precursor protein by presenilin during *Drosophila* development. *EMBO Report* **5**, 405–411.

Magliery T. J., Wilson C. G., Pan W., Mishler D., Ghosh I., Hamilton A. D. and Regan L. (2005) Detecting protein–protein interactions with a green fluorescent protein fragment reassembly trap: scope and mechanism. *J. Am. Chem. Soc.* **127**, 146–157.

Masliah E., Westland C. E., Rockenstein E. M., Abraham C. R., Mallory M., Veinberg I., Sheldon E. and Mucke L. (1997) Amyloid precursor proteins protect neurons of transgenic mice against acute and chronic excitotoxic injuries *in vivo*. *Neuroscience* **78**, 135–146.

Matsuda S., Giliberto L., Matsuda Y., Davies P., McGowan E., Pickford F., Ghiso J., Frangione B. and D'Adamio L. (2005) The familial dementia BRI2 gene binds the Alzheimer gene amyloid-β precursor protein and inhibits amyloid-β production. *J. Biol. Chem.* **280**, 28 912–28 916.

McPhie D. L., Coopersmith R., Hines-Peralta A., Chen Y., Ivins K. J., Manly S. P., Kozlowski M. R., Neve K. A. and Neve R. L. (2003) DNA synthesis and neuronal apoptosis caused by familial Alzheimer disease mutants of the amyloid precursor protein are mediated by the p21 activated kinase PAK3. *J. Neurosci.* **23**, 6914–6927.

Mucke L., Abraham C. R., Ruppe M. D., Rockenstein E. M., Toggas S. M., Mallory M., Alford M. and Masliah E. (1995) Protection against HIV-1 gp120-induced brain damage by neuronal expression of human amyloid precursor protein. *J. Exp. Med.* **181**, 1551–1556.

Mucke L., Masliah E., Johnson W. B., Ruppe M. D., Alford M., Rockenstein E. M., Forss-Petter S., Pietropaolo M., Mallory M. and Abraham C. R. (1994) Synaptotrophic effects of human amyloid β protein precursors in the cortex of transgenic mice. *Brain Res.* **666**, 151–167.

Nofziger D., Miyamoto A., Lyons K. M. and Weinmaster G. (1999) Notch signaling imposes two distinct blocks in the differentiation of C2C12 myoblasts. *Development* **126**, 1689–1702.

Oh S. Y., Ellenstein A., Chen C. D., Hinman J. D., Berg E. A., Costello C. E., Yamin R., Neve R. L. and Abraham C. R. (2005) Amyloid precursor protein interacts with notch receptors. *J. Neurosci. Res.* **82**, 32–42.

Ozalp C., Szczesna-Skorupa E. and Kemper B. (2005) Bimolecular fluorescence complementation analysis of cytochrome P450 2C2, 2E1 and NADPH-cytochrome P450 reductase molecular interactions in living cells. *Drug Metab. Dispos.* **33**, 1382–1390.

Rohn T. T., Ivins K. J., Bahr B. A., Cotman C. W. and Cribbs D. H. (2000) A monoclonal antibody to amyloid precursor protein induces neuronal apoptosis. *J. Neurochem.* **74**, 2331–2342.

Scheuermann S., Hambsch B., Hesse L., Stumm J., Schmidt C., Beher D., Bayer T. A., Beyreuther K. and Multhaup G. (2001) Homodimerization of amyloid precursor protein and its implication in the amyloidogenic pathway of Alzheimer's disease. *J. Biol. Chem.* **276**, 33 923–33 929.

Schroeter E. H., Kisslinger J. A. and Kopan R. (1998) Notch-1 signalling requires ligand-induced proteolytic release of intracellular domain. *Nature* **393**, 382–386.

Selkoe D. and Kopan R. (2003) Notch and presenilin: regulated intramembrane proteolysis links development and degeneration. *Annu. Rev. Neurosci.* **26**, 565–597.

Selkoe D. J., Podlisny M. B., Joachim C. L., Vickers E. A., Lee G., Fritz L. C. and Oltersdorf T. (1988) β-Amyloid precursor protein of Alzheimer disease occurs as 110- to 135-kilodalton membrane-associated proteins in neural and nonneural tissues. *Proc. Natl Acad. Sci. USA* **85**, 7341–7345.

Stockklausner C. and Klocker N. (2003) Surface expression of inward rectifier potassium channels is controlled by selective Golgi export. *J. Biol. Chem.* **278**, 17 000–17 005.

Szczesna-Skorupa E., Mallah B. and Kemper B. (2003) Fluorescence resonance energy transfer analysis of cytochromes P450 2C2 and 2E1 molecular interactions in living cells. *J. Biol. Chem.* **278**, 31 269–31 276.

Van Nostrand W. E., Wagner S. L., Farrow J. S. and Cunningham D. D. (1990) Immunopurification and protease inhibitory properties of protease nexin-2/amyloid β-protein precursor. *J. Biol. Chem.* **265**, 9591–9594.

Vooijs M., Schroeter E. H., Pan Y., Blandford M. and Kopan R. (2004) Ectodomain shedding and intramembrane cleavage of mammalian Notch proteins is not regulated through oligomerization. *J. Biol. Chem.* **279**, 50 864–50 873.

Walter M., Chaban C., Schutze K. *et al.* (2004) Visualization of protein interactions in living plant cells using bimolecular fluorescence complementation. *Plant J.* **40**, 428–438.

Wang Y. and Ha Y. (2004) The X-ray structure of an anti-parallel dimer of the human amyloid precursor protein E2 domain. *Mol. Cell* **15**, 343–353.

Weidemann A., Konig G., Bunke D., Fischer P., Salbaum J. M., Masters C. L. and Beyreuther K. (1989) Identification, biogenesis, and localization of precursors of Alzheimer's disease A4 amyloid protein. *Cell* **57**, 115–126.

Yoon K. and Gaiano N. (2005) Notch signaling in the mammalian central nervous system: insights from mouse mutants. *Nat. Neurosci.* **8**, 709–715.

